Fungal Biology 129 (2025) 101565

Contents lists available at ScienceDirect

Fungal Biology

journal homepage: www.elsevier.com/locate/funbio

The candidate transcription factors PnAtfA, PnCrz1, and PnVf19 contribute to fungal morphogenesis, abiotic stress tolerance, and pathogenicity in the wheat pathogen *Parastagonospora nodorum*

Roya Choupannejad [a,b,*], Bahram Sharifnabi [a], Jérôme Collemare [b], Javad Gholami [a], Rahim Mehrabi [c,d]

[a] Department of Plant Protection, College of Agriculture, Isfahan University of Technology, Isfahan, Iran
[b] Westerdijk Fungal Biodiversity Institute, Uppsalalaan 8, 3584 CT, Utrecht, The Netherlands
[c] Department of Biotechnology, College of Agriculture, Isfahan University of Technology, Isfahan, Iran
[d] Keygene N.V., P.O. Box 216, Wageningen, 6700 AE, The Netherlands

ARTICLE INFO

Handling Editor: Dr S Bates

Keywords:
Virulence
Septoria nodorum leaf and glume blotch
Oxidative and osmotic stress response
Gene knockout

ABSTRACT

The necrotrophic fungus *Parastagonospora nodorum*, the causal agent of wheat glume blotch, is responsible for substantial economic losses in many wheat-growing regions. Despite the high number of transcription factor (TF)-encoding genes in the genome of *P. nodorum*, very little is known about their regulatory functions. Here, we assessed the role of three TFs in the regulation of *P. nodorum* virulence on wheat. We identified encoded in the genome of *P. nodorum* PnAtfA, PnCrz1, and PnVf19, homologous candidate TFs to *Schizosaccharomyces pombe* Atf1, *Saccharomyces cerevisiae* CRZ1, and *S. cerevisiae* Msn2, respectively. Targeted gene replacement of each gene led to reduced mycelial vegetative growth and loss of pathogenicity on wheat. Deletion of *PnAtfA* resulted in phenotype alteration with *ΔPnCrz1* deletion mutants displayed abnormal colony morphology characterized by dense hyphal branching and loss of aerial hyphae development, showing that both PnAtfA and PnCrz1 regulate fungal morphogenesis. Additionally, deletion of *PnAtfA and PnVf19* genes abolished pycnidiospore production whereas Δ*PnCrz1* produced fewer pycnidiospores compared to the wild type. Furthermore, Δ*PnCrz1* and Δ*PnVf19* deletion mutants demonstrated increased sensitivity to hydrogen peroxide showing their involvement in oxidative stress response. The Δ*PnVf19* deletion mutants exhibited increased sensitivity to sodium chloride, suggesting that PnVf19 is essential for osmotic tolerance response. Taken together, these findings suggest that the selected candidate TFs play a key role in the fungal morphogenesis, sporulation, oxidative and osmotic stress tolerance response, and full virulence in *P. nodorum*.

1. Introduction

The necrotrophic fungus *P. nodorum*, is responsible for septoria nodorum leaf and glume blotch (SNB) on wheat, one of the major threats to wheat production worldwide (Duba et al., 2018; Oliver et al., 2012). *P. nodorum* serves as a model organism for studying the pathogenesis of necrotrophic pathogens through the secretion of proteinaceous necrotrophic effectors (NEs) interacting with host susceptibility genes (Oliver et al., 2012). Five NE genes (*SnToxA*, *SnTox1*, *SnTox3*, *SnTox5*, and *SnTox267*) and three wheat S genes (*Tsn1*, *Snn1*, and *Snn3-D1*) have been cloned and studied at the molecular level to date (Peters Haugrud et al., 2022). The NE genes *SnToxA*, *SnTox1* and *SnTox3* are the key pathogenicity determinants in *P. nodorum* causing necrosis in wheat cultivars possessing dominant susceptibility genes *Tsn1*, *Snn1*, and *Snn3-B1*, respectively (Oliver et al., 2012). Three transcription factors (TFs) were found to regulate the expression of these NE genes, and thus pathogenicity. The TF gene *SnStuA*, regulates the expression of *SnTox3* and is required for mycelial growth, carbon metabolism and sporulation in *P. nodorum* (IpCho et al., 2010). The Zn2Cys6 TF gene *PnPf2* regulates the expression of both *SnToxA* and *SnTox3* (Rybak et al., 2017), as well as plant cell wall degradation and twelve effector-like encoding genes (Jones et al., 2019). Also, it has been recently found that PnPf2 has a direct role in the expression regulation other TF genes in *P. nodorum* through direct binding of PnPf2 on the promoter region of TF genes

* Corresponding author. Department of Plant Protection, College of Agriculture, Isfahan University of Technology, Isfahan, Iran.
E-mail address: r.choupannejad@wi.knaw.nl (R. Choupannejad).

https://doi.org/10.1016/j.funbio.2025.101565
Received 14 September 2024; Received in revised form 4 March 2025; Accepted 6 March 2025
Available online 8 March 2025

(John et al., 2024). The C2H2 TF gene *PnCon7* regulates *SnTox3* expression by direct binding to the promotor region of *SnTox3* and also regulates *SnToxA* and *SnTox1* expression (Lin et al., 2018).

A previous study identified six candidate TF genes that were up-regulated in starvation media lacking both nitrogen and carbon sources as well as during the early stages of infection (Choupannejad et al., 2023), and since these findings were coherent with the *P. nodorum* transcriptome data obtained earlier under *in vitro* and *in planta* conditions (Ipcho et al., 2012), we proposed that the candidate TFs play a role in regulating *P. nodorum* pathogenicity (Choupannejad et al., 2023). While two of these candidate TFs are predicted to be part of secondary metabolite gene clusters, the four other ones are homologous to well-characterized fungal TFs including two putative bZIP-type protein-encoding genes in the loci JI435_056770 and JI435_049640, denoted *PnAtfA* and *PnMetR*, sharing homology to the characterized Atf1 in fission yeast, *Schizosaccharomyces pombe* and *ScMetRS* in *Saccharomyces cerevisiae*, respectively and two zinc finger C2H2 type candidate TF genes in the loci JI435_152130 and JI435_037800 designated *PnCrz1* and *PnVf19*, sharing homology to the characterized CRZ1 and Msn2 in *S. cerevisiae*, respectively.

The basic-region leucine zipper-type (bZIP) TF gene *Atf1* has been extensively studied in the fission yeast, *S. pombe* (Wilkinson et al., 1996) and it is known to function downstream of the stress- and mitogen-activated protein kinases (SAPK) cascade which is crucial for osmotic stress responses (Temme et al., 2012). The homologs of Atf1 have been characterized in many fungal species including Moatf1 in *Pyricularia oryzae* (Guo et al., 2010), VDAG_08676 in *Verticillium dahliae* (Fang et al., 2017), BcAtf1 in *Botrytis cinerea* (Temme et al., 2012), CPTF1 in *Claviceps purpurea* (Nathues et al., 2004), CsAtf1 in *Colletotrichum siamense* (Song et al., 2022), PdatfA in *Penicillium digitatum* (Luo et al., 2022), Fgatf1 in *Fusarium graminearum* (Van Nguyen et al., 2013), and FvatfA in *Fusarium verticillioides* (Szabó et al., 2020).

The C2H2 calcineurin-responsive zinc finger 1 (CRZ1) have been studied in *S. cerevisiae* and *S. pombe* (Prz1) in which it regulates genes involved in the Ca^{2+}/calcineurin signaling pathway such as ATPase PMC1 (Hirayama et al., 2003; Matheos et al., 1997). The TF CRZ1 plays a key role in cell wall maintenance in numerous fungi (Schumacher et al., 2008; Yang et al., 2022). Following rising the cytosolic Ca^{2+} level, calcineurin is activated, which in turn dephosphorylates the TF CRZ1 leading to regulating the expression of genes responsible for cell wall biosynthesis and ion homeostasis (Zhang et al., 2013). A key part of how CRZ1 is regulated by dephosphorylation is the binding of calcineurin to the PXIXIT motif, which is known as calcineurin-docking domain (Schumacher et al., 2008). The homologs of CRZ1 have been characterized in other fungi, including MoCRZ1 in *P. oryzae* (Kim et al., 2010), FgCrz1A in *F. graminearum* (Chen et al., 2019), CrzA in *Aspergillus nidulans* (Spielvogel et al., 2008), AaCrz1 in *Alternaria alternata* (Yang et al., 2022), CrzA in *Aspergillus fumigatus* (Soriani et al., 2008), PdCrz1 in *P. digitatum* (Zhang et al., 2013), and BcCrz1 in *B. cinerea* (Schumacher et al., 2008).

The Msn2 C2H2 TF was first characterized in the yeast model *S. cerevisiae* and it has been identified as a general stress-response regulator of the high osmolarity glycerol (HOG) pathway and is important for coping with a wide range of environmental and physiological stresses (Chang et al., 2011; Ruis and Schüller, 1995). HOG1 mitogen-activated protein kinase and histidine kinase signaling pathways have been shown to play a key role in stress tolerance response in *P. nodorum* (John et al., 2016). The homologs of Msn2 such as AbVf19 in *Alternaria brassicicola* (Srivastava et al., 2012), ZtVf1 in *Zymoseptoria tritici* (Mohammadi et al., 2017), VdMsn2 in *V. dahliae* (Tian et al., 2017), MsnA in *Aspergillus parasiticus* and *Aspergillus flavus* (Chang et al., 2011), BcMsn2 in *B. cinerea* (Lu et al., 2023), and MoMsn2 in *P. oryzae* (Zhang et al., 2014) have been characterized.

It has been reported that Atf1, CRZ1, and Msn2 play a significant role in a variety of biological processes such as sporulation, hyphal growth, abiotic stress tolerance, activity of extracellular enzymes, secondary metabolite biosynthesis, and pathogenicity across fungi. The function of these three candidate TFs in other plant pathogens and their expression profile during wheat infection and nutrient starvation suggest that the homologs in *P. nodorum* may play an important role in the pathogenicity and stress tolerance response of this fungus. This study aimed to determine the function of candidate TF genes *PnAtfA*, *PnCrz1*, and *PnVf19* in *P. nodorum* isolate SN15 using targeted gene replacement, and provide new insights into the infection process of this pathogenic fungus on wheat.

2. Materials and methods

2.1. Fungal isolate, media, and growth condition

The reference *P. nodorum* isolate SN15 obtained from Australian Centre for Necrotrophic Fungal Pathogens (ACNFP), Curtin University, Western Australia was used as wild-type (WT) strain in this study. WT strain and candidate TF gene deletion mutants were routinely grown on CzV8CS agar ($NaNO_3$, 2 g/L; KCl, 0.5 g/L; $MgSO_4$, 0.5 g/L; $FeSO_4$, 0.01 g/L; K_2HPO_4, 1 g/L; sucrose, 30 g/L; $CaCO_3$, 3 g/L; V8 juice, 200 mL; agar, 15 g/L; adjusted to pH 6) and minimal media (MM) (sucrose, 30 g/L; $NaNO_3$, 2 g/L, K_2HPO_4; 1 g/L, KCl, 0.5 g/L; $MgSO_4 \cdot 7H_2O$, 0.5 g/L; $ZnSO_4 \cdot 7H_2O$, 0.01 g/L; $FeSO_4 \cdot 7H_2O$, 0.01 g/L; $CuSO_4 \cdot 5H_2O$ 2.5 mg/L; adjusted to pH 6) (Chooi et al., 2015a) at 22 °C. To stimulate pycnidia development CzV8CS plates were incubated under alternating 12-h NUV photoperiod/12-h darkness for three weeks.

2.2. Characterization and phylogenetic analysis of candidate transcription factor (TF) genes

The amino acid sequence of *P. nodorum* SN15 candidate TFs PnAtfA, PnCrz1, and PnVf19 obtained from BioProject ID PRJNA686477 (https://www.ncbi.nlm.nih.gov/bioproject/PRJNA686477) were used to perform a homology search using the NCBI BlastP tool in order to retrieve full protein sequences of both characterized and putative homologous TFs from taxonomically diverse fungal classes. The obtained protein sequences were used to build phylogenetic trees in MEGA v.11 (Tamura et al., 2021); alignment was done with ClustalW algorithm, trimmed manually and phylogenetic trees were contructed based on the neighbor-joining (NJ) method with 1000 bootstrap replicates. The conserved domains of characterized homologs of candidate TF genes were identified using InterProScan (https://www.ebi.ac.uk/interpro/).

2.3. Generation of candidate TF gene deletion constructs

To generate the candidate TF gene deletion constructs, the Multisite Gateway ™ cloning strategy (Thermo Fisher Scientific, Waltham, MA) was used. Briefly, approximately 1 kb of DNA from the upstream and downstream flanking region of TF genes were employed as homologous recombination sites for deletion of TF genes and replacement with the hygromycin phosphotransferase (*hph*) gene as a selection marker.

The upstream flanking regions of candidate TF genes *PnAtfA*, *PnCrz1*, and *PnVf19* were amplified with primer pairs PnATFA-CE11 (F/R), PnCrz1-CE11 (F/R), and PnVf19-CE11 (F/R) (Table S1), respectively each containing 21-bp sequences homologous to *pRM236* plasmid (Mehrabi et al., 2015) to introduce overlapping regions with the cleavage site in *pRM236* entry vector digested by *Sal*I. All PCR fragments were amplified using Phusion ™ High-Fidelity DNA Polymerase (Thermo Scientific Cat. No. F530S) based on the manufacturer's protocol. One microgram of *pRM236* plasmid was linearized with 5 U *Sal*I (Promega Cat. No. R6051) for 4 h at 37 °C to generate a compatible overhang with the PCR fragments. Afterward, 20 ng of upstream flanking fragments were cloned into 100 ng of *pRM236* plasmid using Clon Express MultiS One Step kit (Vazyme Cat. No. C113) in accordance with manufacturer's instructions.

The downstream flanking regions of candidate TF genes *PnAtfA*,

PnCrz1, and *PnVf19* were amplified using primer pairs PnATFA-GW2 (F/R), PnCrz1-GW2 (F/R), and PnVf19-GW2 (F/R) (Table S1), respectively to introduce *attB2* and *attB3R* Gateway flanking regions. About 50 ng of PCR products were cloned into 100 ng *pDONR^{TM} P2R-P3* using one microliter of Gateway™ BP Clonase™ II Enzyme mix (Invitrogen™ by Thermo Fisher Scientific Cat. No. 11789020) according to the manufacturer's instructions. To generate the TF gene deletion constructs, 150 ng of entry vector *pRM236* and 100 ng of *pDONR^{TM} P2R-P3* along with 140 ng of the entry vector *pRM250* containing the *hph* selection marker cassette (Mehrabi et al., 2015) were mixed with 130 ng of destination vector *pPm4*3 GW in a Multisite Gateway™ cloning mixture using one microliter Gateway™ LR Clonase™ II Enzyme mix (Invitrogen™ by Thermo Fisher Scientific Cat. No. 11791020) based on the manufacturer's protocol.

Each cloning reaction was directly introduced into chemically competent *Escherichia coli* DH5α cells. Positive bacterial colonies carrying the expected construct were identified through colony PCR with both general (M13 F/R) and specific primer pairs (Table S1) using GoTaq® G2 Hot Start Taq Polymerase (Promega Cat. No. M7405). Finally, the resulting gene deletion plasmids were linearized with 5 U of restriction enzyme *Kpn*I (Promega Cat. No. R6341) for 4 h at 37 °C. Plasmids were isolated in small and medium scales using the PureLink™ Quick Plasmid Miniprep (Invitrogen™ by Thermo Fisher Scientific Cat. No. K210011) and PureLink™ HiPure Plasmid Midiprep (Invitrogen™ by Thermo Fisher Scientific Cat. No. K210005), respectively, according to the manufacturer's instruction. PCR fragments and linearized plasmids were purified using NucleoSpin Gel and PCR Clean-up kit (Macherey–Nagel Cat. No. 740609.50) according to the manufacturer's instruction. The insertion of desired fragment into the plasmids were verified by sequencing (Macrogen, Europe).

2.4. Preparation of *P. nodorum* protoplasts

The preparation of *P. nodorum* protoplasts was conducted as described previously (Solomon et al., 2004b) with some modifications. Briefly, a 250 mL flask with 50 mL CzV8CS liquid media supplemented with 2.5 mL filter-sterilized complete supplement (Bacto-casamino acids, 20 g/L; Bacto-peptone, 20 g/L; Bacto-yeast extract, 20 g/L; Adenine, 3 g/L; Biotin, 0.02 g/L; Nicotinic acid, 0.02 g/L; P-aminobenzoic acid, 0.02 g/L; Pyridoxine, 0.02 g/L; Thiamine, 0.02 g/L) was inoculated with 2 mL of *P. nodorum* isolate SN15 spore suspension (10^7 spore/mL) and incubated in a shaking incubator (140 rpm, 22 °C) for 24 h. Mycelia were harvested by centrifuging at 4000×*g* for 10 min at 4 °C, and were washed using 25 mL 0.8 M NaCl (4000×*g*, 5 min, 4 °C). Afterward, mycelia were resuspended in one 50 mL tube, containing 10 mL filter-sterilized protoplasting mix solution (Glucanex® (Sigma Aldrich Cat. No. L1412), 200 mg; Driselase™ Basidiomycetes sp (Sigma Aldrich Cat. No. D8037), 50 mg; dissolved in 10 mL of 0.8 M NaCl) and incubated for 2.5 h in a shaking incubator with gentle agitation (100 rpm, 30 °C). The protoplast suspension was filtered through two layers of miracloth and centrifuged at 3000×*g*, 5 min, 4 °C. The supernatant was discarded and the protoplasts were resuspended in 3 mL STC (1.2 M sorbitol, 10 mM Tris–HCl, pH 7.5, 10 mM $CaCl_2$) buffer. The concentration of the protoplast suspension was adjusted to 10^7 protoplast/mL using a hemocytometer.

2.5. Transformation of *P. nodorum* with candidate TF gene deletion constructs

The gene deletion constructs were transformed into the *P. nodorum* SN15 protoplasts as described previously (Solomon et al., 2004b) with some modifications. Three microliters of linearized deletion construct (4 μg/μL) were dissolved in 7 μL STC buffer and was added to 100 μL of protoplast suspension followed by incubation on ice for 5 min. One milliliter of filter-sterilized 60 % (wt/vol) polyethylene glycol 4000, 10 mM $CaCl_2$, 0.8 M NaCl in 5 mM Tris–HCl (pH 7.5) was added to the mixture followed by gentle inversion of the suspension and incubation of 20 min at room temperature. The transformation mixture was added to 10 mL pre-warmed (50 °C) CzV8-top agar (Czapek-Dox liquid, 45.4 g/L; sorbitol, 182.2 g/L; filtered V8 juice, 200 mL; Oxoid agar, 7.5 g/L; adjusted to pH 6), mixed by gentle inversion, and was poured onto plates containing 10 mL CzV8-proto agar (Czapek-Dox liquid, 45.4 g/L; sorbitol, 182.2 g/L; filtered V8 juice, 200 mL; Oxoid agar, 10 g/L; adjusted to pH 6). The plates were wrapped in aluminum foil and kept in 22 °C for 40 h. Afterward, the CzV8-proto agar plates were overlaid with an additional 10 mL of CzV8-proto agar containing 60 μL of hygromycin (InvivoGen Cat. No. ant-hg-1) stock solution (100 mg/mL) to achieve a final concentration of 200 μg/mL for the entire plate. After ten days incubation in darkness at 22 °C, transformants were sub-cultured on fresh CzV8CS containing 200 μg/mL hygromycin. Homologous integration of transformants was assessed *via* diagnostic PCR using specific primer pairs (Table S1 and Fig. S1). The transformants were screened to achieve at least three independent mutants for each candidate TF gene.

2.6. *Hph* gene copy number

To determine the *hph* gene copy number in the TF gene deletion mutants together with ectopic strains, a quantitative real-time PCR (q-RT PCR) assays using the $2^{-\Delta\Delta Ct}$ method was employed (Schmittgen and Livak, 2008; Solomon et al., 2008). The q-RT PCR assay was done in a LightCycler® 480 (Roche, Switzerland) apparatus using a PowerUp™ SYBR™ Green master mix (Applied Biosystems™, Cat. No. A25742) with the following program; initial denaturation of 95 °C for 3 min followed by 40 cycles of 95 °C for 10 s, annealing of 57 °C for 10 s, and extension of 72 °C for 20 s. The *hph* gene copy number was evaluated through the normalization of the *hph* gene (amplified using Hyg_qpcr F/R primers, Table S1) copy number against the single copy genes γ-actin (amplified using Act1 F/R primers, Table S1) and elongation factor 1α (amplified using EF1α F/R primers, Table S1).

2.7. *In vitro* phenotyping

The phenotyping characterization (colony morphology, growth, sporulation, oxidative, ionic, and osmotic stress response) was assessed for three independent TF gene deletion mutants along with one ectopic transformant and a wild type (WT) control in triplicates. To compare the growth rate, the fungal colony diameter grown on CzV8CS and MM were measured 10 days post inoculation. For sporulation assay, strains were grown on CzV8CS for three weeks under alternating 12-h NUV photoperiod/12-h darkness. Plates were washed with 5 mL of sterile distilled water and the pycnidiospores were scraped with a sterile scalpel, passed through two layers of miracloth, then counted using a haemocytometer.

The oxidative tolerance response of *ΔPnAtfA*, *ΔPnCrz1*, and *ΔPnVf19* deletion mutants compared to ectopic and WT strains was determined by culturing the fungi on MM containing 0 and 2 mM hydrogen peroxide (H_2O_2), and measuring the radial growth of strains 10 days post inoculation as described previously (Chooi et al., 2015b). To evaluate the role of candidate TFs under ionic stress, the fungal radial growth was measured 10 days after inoculation on MM containing 0 and 100 mM $CaCl_2$ (Spielvogel et al., 2008). The ability of TF deletion mutants to grow under hyperosmotic condition was assessed by comparing their radial growth on MM media supplemented with concentration of 0 and 0.5 M NaCl (Lowe et al., 2008). The relative colony diameters (e.g. diameter 2 mM/0 mM H_2O_2) were used for statistical analysis.

2.8. Statistical analysis

All experiments were carried out in triplicates and to evaluate the significant difference among treatments, a one-way ANOVA followed by Tukey's multiple comparison test (alpha 0.05) was performed using GraphPad Prism (v.10.2.3) for windows (www.graphpad.com).

2.9. Pathogenicity assay

Detached leaf assays (DLAs) were performed as described previously (Solomon et al., 2004a) to evaluate the virulence of each candidate TF gene mutants compared to the WT and ectopic strains in three replications. Fourteen-day old wheat leaves (cultivar Grandin) were cut in fragments of 10 cm long, surface sterilized with 70 % ethanol solution, followed by rinsing in sterile distilled water, and were placed on 1 % water agar plates with the ends of the leaves embedded into the agar. Agar plugs containing mycelium from 5-day old CzV8CS plates were placed on the leaf surface after applying 5 µL of 0.02 % Tween 20 to improve the adhesion of the mycelium. The plates were incubated for five days in a photoperiod of 12 h light/12 h darkness at 22 °C to develop SNB symptoms.

3. Results

3.1. Sequence and phylogenetic analysis of PnAtfA, PnCrz1, and PnVf19 predicted transcription factors

PnAtfA (JI435_056770), PnCrz1 (JI435_152130) and PnVf19 (JI435_037800) were previously identified in *P. nodorum* SN15 as homologs of *S. pombe* Atf1, *S. cerevisiae* CRZ1, and *S. cerevisiae* Msn2 TFs, respectively (Choupannejad et al., 2023). *PnAtfA* is located on chromosome 6 of *P. nodorum* SN15 and its open reading frame (ORF) spans 2482 bp interrupted by five introns, encoding a 541 amino acid protein. PnAtfA possesses one bZIP conserved domain (IPR004827) showing 100 % homology to the bZIP domain of *A. alternata* AaAtf1 (Fig. S2 A), two Aft1_HRR domains (IPR021755-56), and one Atf1-OSM domain (IPR020956). *PnCrz1* is located on chromosome 8 comprising an ORF of 2706 bp interrupted by three introns and encodes for an 854 amino acid protein. It features two Znf_C2H2_type conserved domains (IPR013087) that share most similarity with the domains found in *A. alternata* AaCrz1 (Fig. S2 B). *PnVf19* is located on chromosome 3 and spans an ORF of 1943 bp that is interrupted by three introns, resulting in the encoding of a 535 amino acid protein. The protein sequence contains a single Znf_C2H2_type conserved domain (IPR013087) which share 100 % identity with the domain found in *A. brassicicola* AbVf19 and *Setosphaeria turcica* StMsn2 (Fig. S2 C).

The phylogenetic analysis showed that PnAtfA, PnCrz1 and PnVf19 TFs were distantly related to the characterized TFs in yeasts *S. pombe* Atf1, *S. cerevisiae* CRZ1, and *S. cerevisiae* Msn2, respectively (Fig. 1). The PnAtfA belongs to the strongly supported clade which includes the characterized *A. alternata* AaAtf1, *P. digitatum* PdAtfA, *A. nidulans* AnAtfA, *V. dahliae* VdAtf1, *Neurospora crassa* NcAtf1, *P. oryzae* MoAtf1, *C. purpurea* CpTf1, *Trichoderma guizhouense* TgAtf1, *Fusarium oxysporum* FoAtf1, *F. graminearum* FgAtf1, and other putative Atf1 homologs, indicating that PnAtfA is orthologous to those characterized TFs (Fig. 1 A). The phylogeny of PnVf19 also shows this TF is orthologous to the characterized *S. turcica* StMsn2, *A. brassicicola* AbVf19, *Z. tritici* ZtVf1, *A. fumigatus* AfSeb1, *A. parasiticus* Msn2, *B. cinerea* BcMsn2, *P. oryzae* MoMsn2, *V. dahliae* VdMsn2, and *Trichoderma atroviride* TaSeb1 (Fig. 1 C). In contrast, PnCrz1 is found in a supported clade with the characterized *A. alternata* AaCrz1and *F. graminearum* FgCrz1A only. Other characterized CRZ1 homologous TFs belong to a different clade and are likely paralogs (Fig. 1 B).

3.2. Targeted deletion of PnAtfA, PnCrz1, and PnVf19

To investigate the role of candidate TF genes *PnAtfA*, *PnCrz1*, and *PnVf19* in *P. nodorum*, we performed targeted gene replacement of each gene. Candidate TF gene deletion and integration of the hygromycin

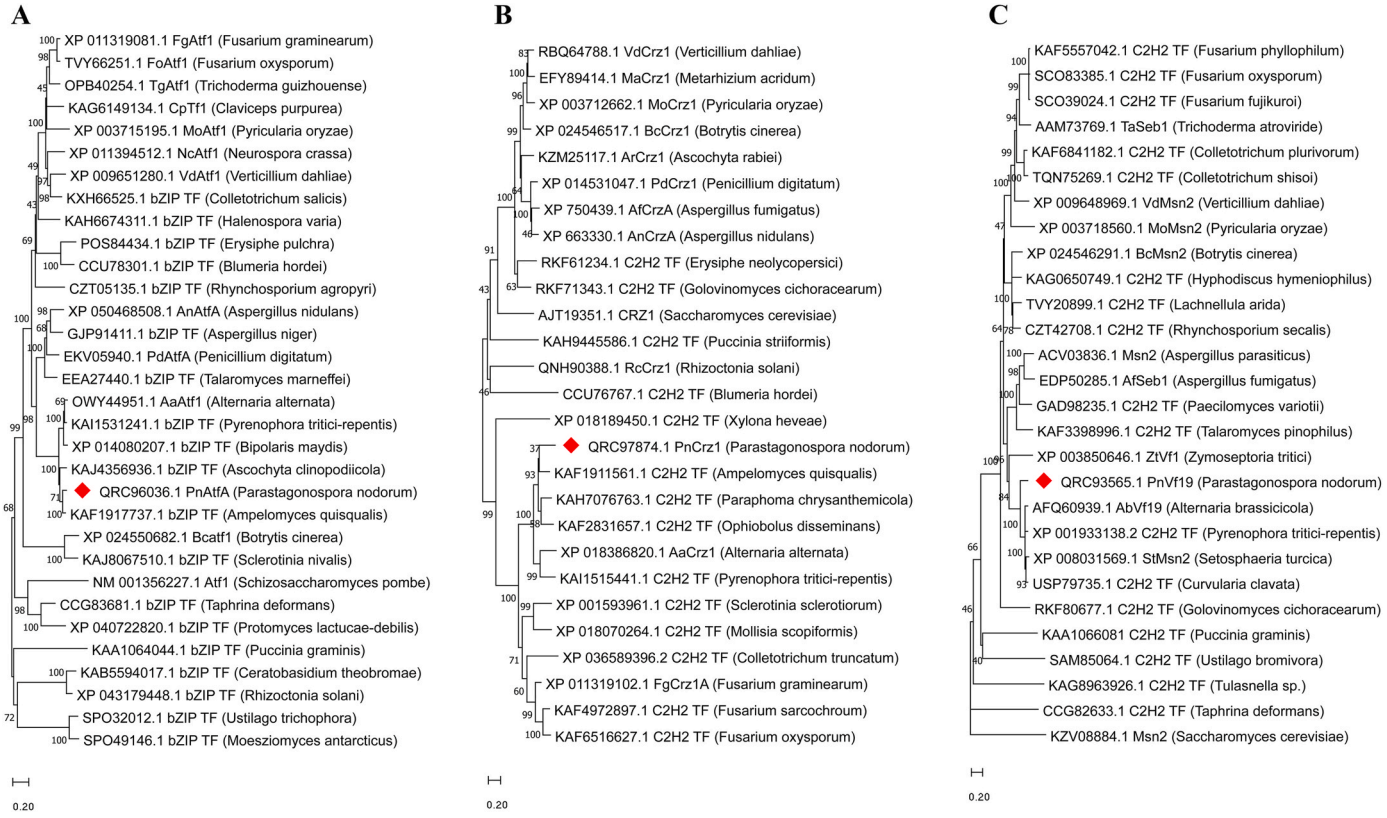

Fig. 1. Phylogenetic analysis of three candidate transcription factors (TFs) in *Parastagonospora nodorum* SN15; phylogenetic tree of characterized and putative homologs of (A) PnAtfA, (B) PnCrz1, and (C) PnVf19. Protein sequences were aligned with ClustalW, and the neighbor-joining method in MEGA v.11 was employed for tree construction, with numbers indicating the percentage occurrence in 1000 bootstrap replicates. The tree is midpoint rooted. The characterized TFs in this study are marked with red diamonds.

phosphotransferase selection marker at the TF gene loci were verified by PCR (Fig. S1). Results confirmed the successful candidate TF gene deletion in three independent mutants for each gene, as indicated by the absence of expected amplicons compared to WT and ectopic strains (Table 1; Figs. S3–S5). The presence of *hph* selection marker in mutants and ectopic integration transformants, but not in WT, confirmed successful marker integration at the TF loci *via* homologous recombination (Figs. S3–S5). All deletion mutants carry a single copy of the *hph* gene, validating the integration of the selection marker at the expected genomic location (Fig. S6). The three ectopic transformants that were kept for further analyses contain up to 10 copies of the *hph* gene (Fig. S6), but none of them integrated at the locus (Figs. S3–S5). Attempts to obtain *PnMetR* deletion mutants were unsuccessful (data not shown), suggesting deletion of this candidate TF is lethal in *P. nodorum* and was not further considered for functional analysis.

3.3. Altered growth of ΔPnAtfA, ΔPnCrz1, and ΔPnVf19 deletion mutants

The vegetative growth on Petri dishes of all candidate TF gene deletion mutants *ΔPnAtfA*, *ΔPnCrz1*, and *ΔPnVf19* was to affect with significantly reduced growth by 20–50 % compared to wild type and ectopic strains, 10 days after inoculation on CzV8CS medium (Fig. 2 A). Morphological characterization on CzV8CS medium showed that *ΔPnAtfA* deletion mutants produced a compact colony with a slight dark ring compared to WT and ectopic strains (Fig. 2 B). *ΔPnCrz1* deletion mutants displayed abnormal colony morphology characterized by producing dense hyphal branching, loss of aerial hyphae development, and the appearance of cracks on the colony surface (Fig. 2 B). Additionally, three weeks after maintaining under sporulation condition (12-h NUV/12-h darkness) the culture media of *ΔPnCrz1* deletion mutants turned to dark orange while no color change was observed in culture media of ectopic and WT strains (Fig. 2 C). In contrast, despite the observed slower growth, the morphology of *ΔPnVf19* deletion mutants appeared identical to WT and ectopic strains (Fig. 2 B).

3.4. PnAtfA, PnCrz1, and PnVf19 are required for sporulation

Δ*PnAtfA* and Δ*PnVf19* deletion mutants failed to produce pycnidia and consequently pycnidiospores even after three weeks of incubation of CzV8CS plates under alternating 12-h NUV photoperiod/12-h darkness (Fig. 3). Δ*PnCrz1* produced about 50 % less pycnidiospores compared to WT and ectopic strains after three weeks of exposure to alternating 12-h NUV photoperiod/12-h darkness (Fig. 3). These results implied the role of the candidate TF genes in asexual development of *P. nodorum*.

3.5. PnCrz1 and PnVf19 are involved in oxidative stress tolerance

Atf1 has been reported to play a role in the osmotic and oxidative stress responses (Wilkinson et al., 1996). Msn2 was also reported to be a general stress-response regulator (Matheos et al., 1997). To assess the oxidative stress response of the three TF gene *ΔPnAtfA*, *ΔPnCrz1*, and *ΔPnVf19* deletion mutants compared to WT and ectopic strains, we exposed these strains to 2 mM H_2O_2. Both ectopic and WT strains were not affected by 2 mM H_2O_2 (Fig. 4). The radial growth of *ΔPnCrz1* and *ΔPnVf19* deletion mutants were significantly reduced under the concentration of 2 mM compared to ectopic and WT strains (Fig. 4 B and 4 C) while *ΔPnAtfA* deletion mutants were not significantly affected (Fig. 4 A) showing that TF genes *PnCrz1* and *PnVf19* confer to oxidative tolerance response.

Table 1
Total number of transformants and true mutants obtained by deletion of candidate transcription factor (TF) genes in *Parastagonospora nodorum* SN15.

TF gene	No. of obtained transformants	No. of screened transformants	No. of obtained true mutants	Deletion rate (%)
PnAtfA	43	15	3	20
PnCrz1	37	13	3	23
PnVf19	52	23	3	13

3.6. PnCrz1 plays a role in calcium signaling response

Since CRZ1 is involved in calcium/calcineurin signaling pathway in *S. cerevisiae* (Matheos et al., 1997) and caused resistance to high concentration of calcium in numerous fungal species such as *B. cinerea* (Schumacher et al., 2008), we tested the radial growth of *ΔPnAtfA*, *ΔPnCrz1*, and *ΔPnVf19* deletion mutants along with ectopic and WT strains on MM containing 100 mM $CaCl_2$. Only *ΔPnCrz1* deletion mutants were affected by high concentration of Ca^{2+} with a significantly reduced growth when compared to ectopic and WT strains (Fig. 5). This observation confirmed that only TF gene *PnCrz1* had a protection role against high concentration of Ca^{2+}.

3.7. PnVf19 plays a role in osmotic tolerance response

The homologs of *PnVf19* are reported to play a role in the osmotic stress response (Chang et al., 2011; Zhang et al., 2014; Mohammadi et al., 2017; Tian et al., 2017). To evaluate if the candidate TFs are also involved in this response in *P. nodorum*, we compared the radial growth of candidate TF deletion mutants, ectopic and WT on media supplemented with concentrations of 0.5 M NaCl (Lowe et al., 2008). WT and ectopic strains did not display any significant decrease in radial growth upon exposure to 0.5 M NaCl (Fig. 6). This observation was consistent with results obtained by Lowe et al. (2008) where no significantly different growth of *P. nodorum* SN15 was found under concentrations of 0.25 M and 0.5 M NaCl (Lowe et al., 2008). Similarly, *ΔPnAtfA* and *ΔPnCrz1* deletion mutants could resist the concentration of 0.5 M NaCl as did ectopic and WT strains (Fig. 6 A and 6 B). In contrast, *ΔPnVf19* deletion mutants show significant reduction in radial growth, suggesting that this candidate TF is required for osmotic tolerance response as reported in other fungi. These results also show that the phenotype observed for *ΔPnCrz1* deletion mutants when grown on media supplemented with $CaCl_2$ is due to calcium signaling and not to a general ionic stress.

3.8. PnAtfA, PnCrz1, and PnVf19 are essential for virulence

The role of candidate TF genes in the virulence of *P. nodorum* was determined using detached-leaf assays. Because all three deletion mutants showed reduced or complete loss of asexual sporulation, pathogenicity assays were performed with mycelium plugs deposited on the leaves with three biological replicates. Five days after inoculation, both ectopic and WT strains induced typical SNB necrotic lesions and hyphal growth was also visible on the agar plugs (Fig. 7). A significant difference in SNB symptom development was observed on detached wheat leaves inoculated with mycelial plugs of candidate TF gene deletion mutants compared to WT and ectopic strains (Fig. 7). While the plug size slightly differs from one sample to another, the WT and ectopic strains did not show any difference in virulence, indicating that it does not impact symptom development. One of the *ΔPnCrz1* deletion mutants produced a very limited chlorosis, but overall *ΔPnAtfA*, *ΔPnCrz1*, and *ΔPnVf19* deletion mutants were found to be unable to produce or provoked weak SNP symptoms on wheat leaves (Fig. 7). This observation indicates that the deletion of *ΔPnAtfA*, *ΔPnCrz1*, and *ΔPnVf19* TF genes attenuates the virulence of *P. nodorum* on wheat.

4. Discussion

The pathogenicity of *P. nodorum* on wheat mainly relies on the production of NEs (Oliver et al., 2012). The regulation of the expression of NE genes was shown to involve three transcription factor that are thus

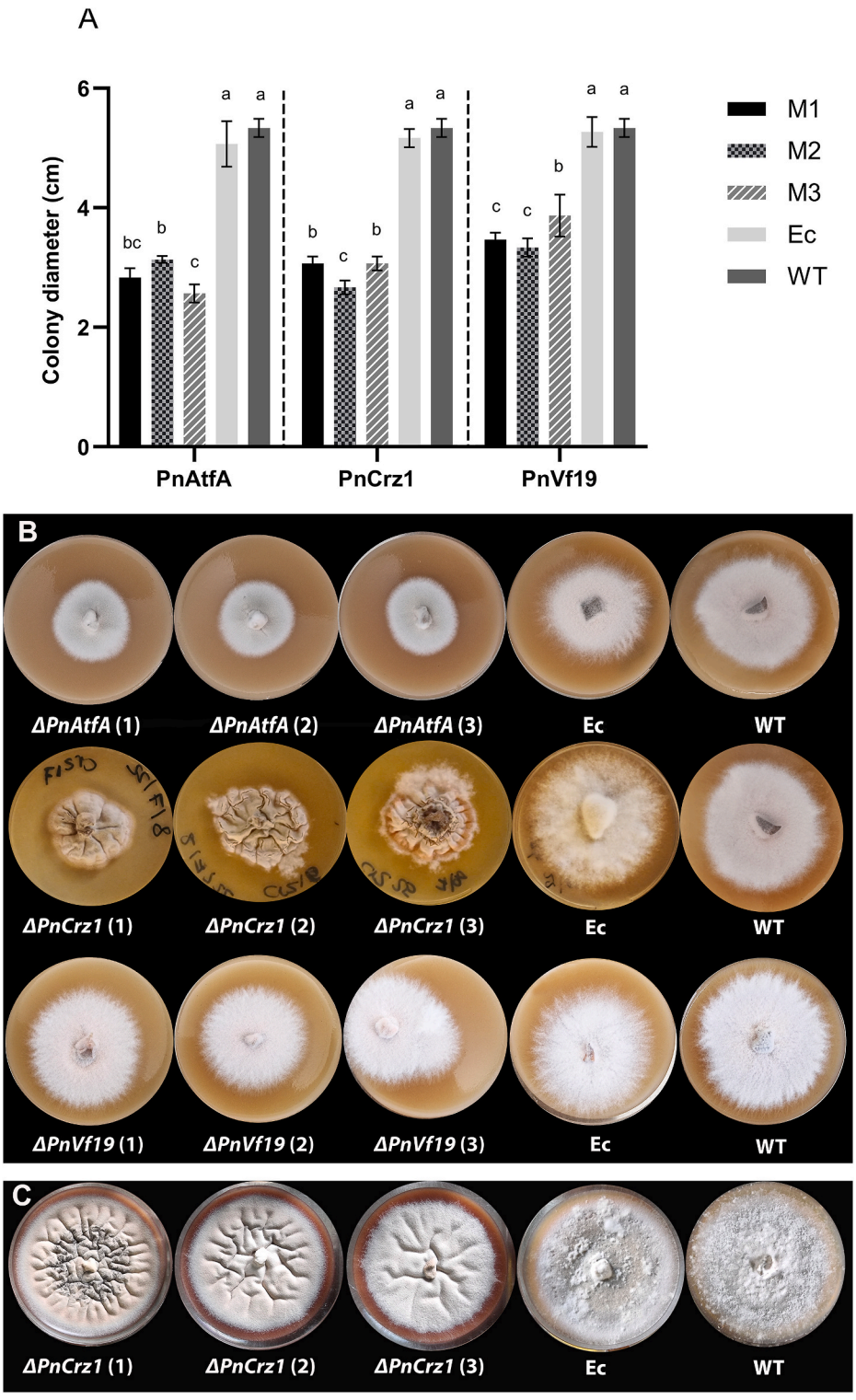

Fig. 2. Characterization of the morphology of Δ*PnAtfA*, Δ*PnCrz1*, and Δ*PnVf19* deletion mutants. (A) Assessment of colony radial growth of three independent transcription factor genes (TFs) Δ*PnAtfA*, Δ*PnCrz1*, and Δ*PnVf19* deletion mutants (M1, M2, and M3) in comparison with ectopic (Ec) and wild type (WT) strains. Error bars represent the standard deviation. Different letters show significantly different values ($p < 0.05$). (B) Morphology of colonies formed by Δ*PnAtfA*, Δ*PnCrz1*, and Δ*PnVf19* deletion mutants compared to Ec and WT strains 10 days post inoculation on CzV8CS. (C) Alterations in the color of the CzV8CS culture medium were noted in three independent Δ*PnCrz1* deletion mutants as compared to Ec and WT strains three weeks after cultivation under 12-h NUV/12-h darkness.

important for virulence (IpCho et al., 2010; Lin, 2017; Rybak et al., 2017). In a previous study, six other candidate TFs were found to be up-regulated during the early stages of wheat infection and nutrient deprivation (Choupannejad et al., 2023). We deleted three of these candidate TFs, *PnAtfA*, *PnCrz1*, and *PnVf19* in *P. nodorum* SN15 to evaluate their involvement in pathogenicity and stress tolerance. The bZIP TF PnAtfA is homolog of Atf1 in the fission yeast *S. pombe* (Fig. 1) and was found to be required for vegetative growth and morphology of *P. nodorum* as Δ*PnAtfA* deletion mutants differed in growth and colony morphology from ectopic and WT strains (Fig. 2). Furthermore, PnAtfA

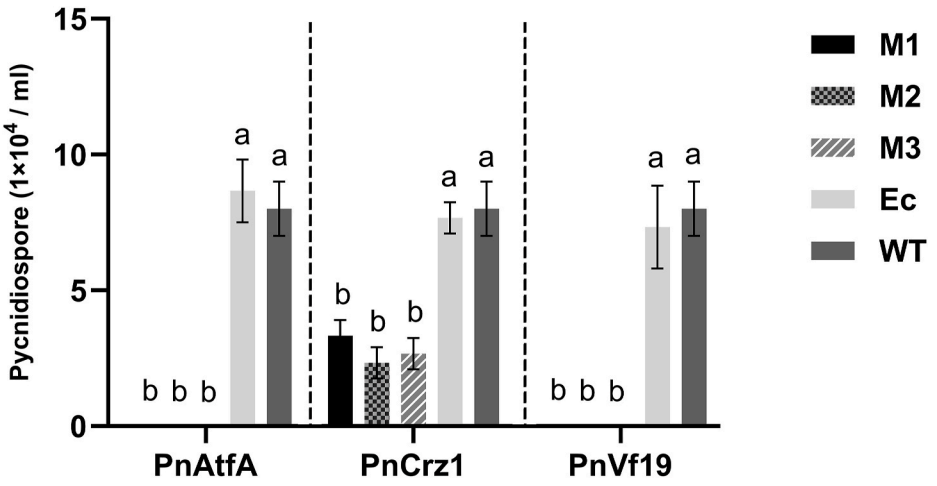

Fig. 3. Assessment of pycnidiospore production in three independent Δ*PnAtfA*, Δ*PnCrz1*, and Δ*PnVf19* deletion mutants (M1, M2, and M3) in comparison with ectopic (Ec) and wild type (WT) strains. Error bars represent the standard deviation. Different letters show significantly different values ($p < 0.05$).

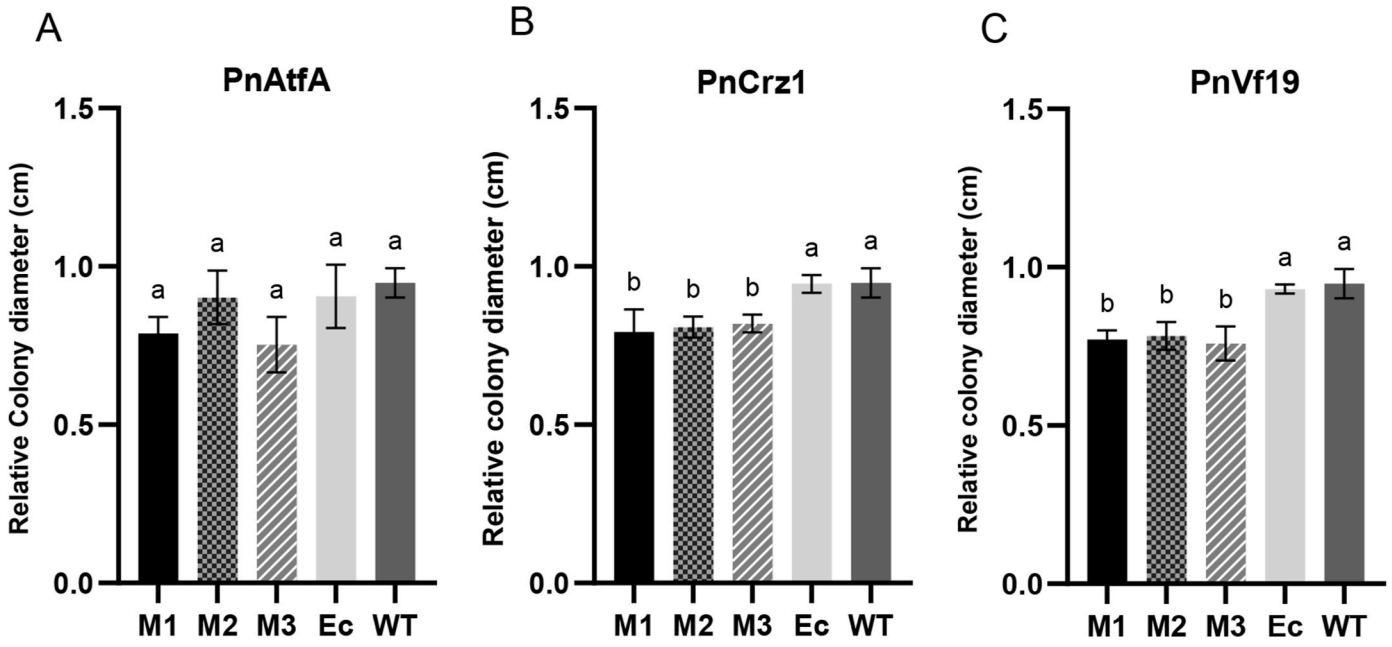

Fig. 4. Oxidative stress tolerance response of (A) Δ*PnAtfA*, (B) Δ*PnCrz1*, and (C) Δ*PnVf19* deletion mutants compared to ectopic (Ec) and wild type (WT) strains. Increased oxidative stress sensitivity of Δ*PnCrz1* (B) and Δ*PnVf19* (C) deletion mutants in comparison with Ec and WT strains when grown on MM containing 2 mM H_2O_2. Δ*PnAtfA* (A) deletion mutants were not significantly affected by oxidative stress. The relative colony diameters were analyzed using a one-way ANOVA followed by Tukey's multiple comparison test. Error bars represent the standard deviation. Different letters show significantly different values ($p < 0.05$).

was shown to play a role in sporulation and pathogenicity of *P. nodorum* with deletion mutants unable to develop pycnidia and induce symptoms on wheat leaves (Figs. 3 and 7). These results align with previous studies evaluating the role of Atf1 homologs in other fungi. For instance, Moatf1 in *P. oryzae* is crucial for fungal growth and pathogenicity (Guo et al., 2010). Likewise, *VDAG_08676*, another *Atf1* homolog has a role in conidial production and virulence in *V. dahliae* (Fang et al., 2017).

Atf1 has been identified as a key player in stress-responsive transcriptional regulation in the yeast *S. pombe* (Wilkinson et al., 1996) and in other fungal species such as *P. oryzae* (Guo et al., 2010) and *C. purpurea* where it acts as a suppressor of host reactive oxygen species (ROS) (Nathues et al., 2004). However, our finding suggests that PnAtfA may not significantly contribute to oxidative and osmotic stress response, as Δ*PnAtfA* mutants did not show significant differences from ectopic and WT strains when exposed to 2 mM H_2O_2 and 0.5 M NaCl, respectively (Figs. 4 and 6). Other studies also indicated that Atf1 homologs do not always influence stress responses; for example, VDAG_08676 in *V. dahliae* is associated with conidial production and virulence, but is not required for oxidative or osmotic stress responses (Fang et al., 2017). Similarly, deletion of *BcAtf1* in *B. cinerea* had no impact on oxidative or osmotic stress responses (Temme et al., 2012), and mycelia of *P. digitatum ΔPdatfA* deletion mutants were unaffected under such conditions (Luo et al., 2022). Interestingly, in some cases, *Atf1* deletion even leads to increased stress resistance rather than causing sensitivity. For instance, deletion of *CsAtf1* enhanced osmotic stress resistance *in C. siamense* (Song et al., 2022). Conversely, *F. graminearum ΔFgatf1* mutants showed increased sensitivity to osmotic stress, but less sensitivity to oxidative stress than WT strains (Van Nguyen et al., 2013). This observation highlights that, while Atf1 is well-known for its role in regulating stress-responsive transcription in yeast and some fungi, there are cases where it either plays no role in the stress response or may even lead to increased sensitivity. These findings

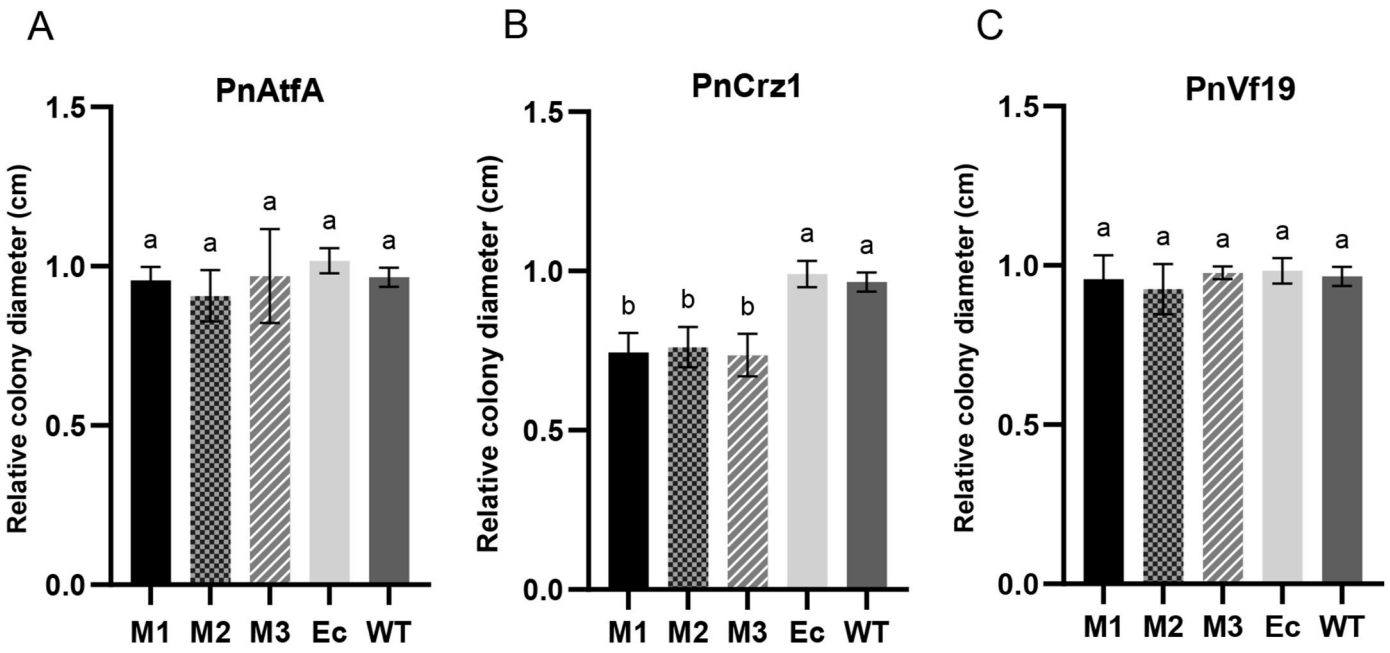

Fig. 5. Ionic stress tolerance response of (A) *ΔPnAtfA*, (B) Δ*PnCrz1*, and (C) Δ*PnVf19* deletion mutants compared to ectopic (Ec) and wild type (WT) strains. Only Δ*PnCrz1* deletion mutants (B) showed a significantly reduced growth rates in comparison with Ec and WT in the minimal media (MM) containing 100 mM $CaCl_2$. The relative colony diameters were analyzed using a one-way ANOVA followed by Tukey's multiple comparison test. Error bars represent the standard deviation. Different letters show significantly different values ($p < 0.05$).

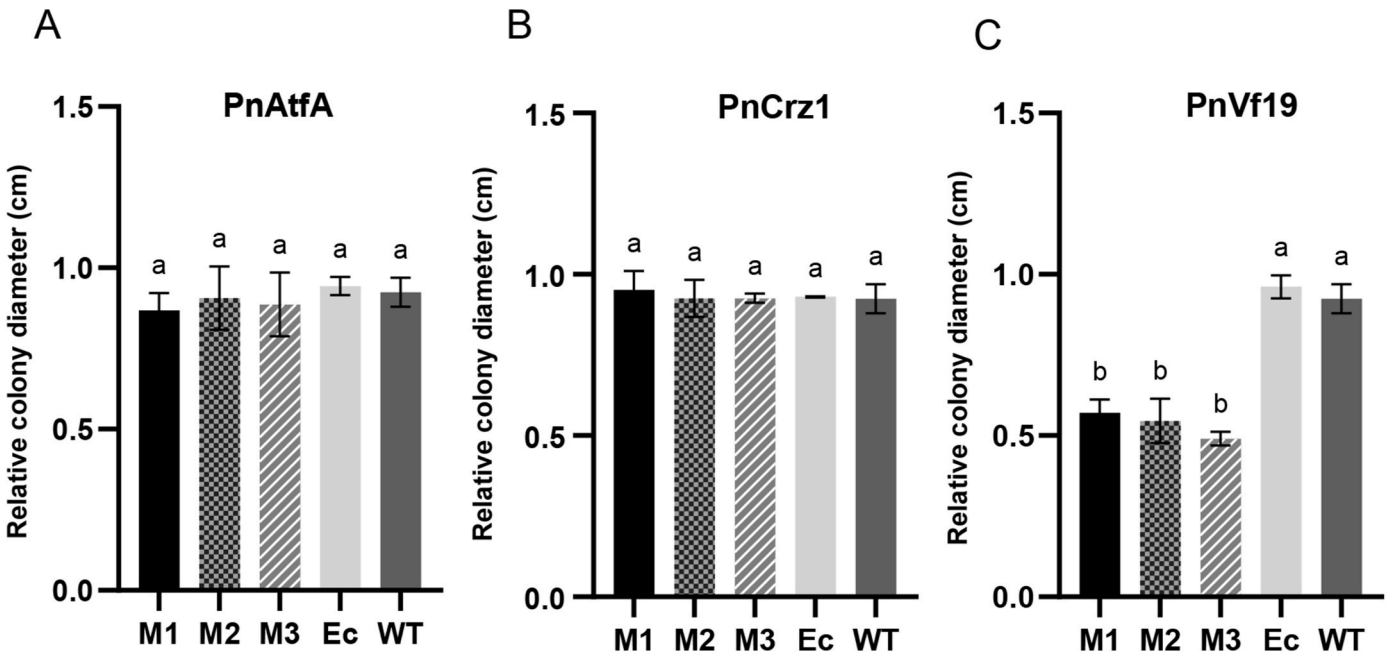

Fig. 6. Osmotic stress tolerance response of (A) *ΔPnAtfA*, (B) Δ*PnCrz1*, and (C) Δ*PnVf19* deletion mutants compared to ectopic (Ec) and wild type (WT) strains. Only Δ*PnVf19* deletion mutants (C) showed increased osmotic stress sensitivity in comparison with Ec and WT strains when grown on MM containing 0.5 M NaCl. The relative colony diameters were analyzed using a one-way ANOVA followed by Tukey's multiple comparison test. Error bars represent the standard deviation. Different letters show significantly different values ($p < 0.05$).

demonstrate the diverse functions of Atf1 homologs in oxidative stress responses across various fungal species (Fang et al., 2017).

The candidate TF gene *PnCrz1* was identified as homologous to the characterized *CRZ1* gene in *S. cerevisiae* (Fig. 1). We observed impaired mycelial growth (Fig. 2), decreased pycnidia production (Fig. 3), diminished oxidative stress tolerance (Fig. 4), sensitivity to high concentrations of Ca^{2+} (Fig. 5) and lack of virulence in *P. nodorum ΔPnCrz1* deletion mutants (Fig. 7). These results implied that PnCrz1 has a role in colony growth and sporulation, tolerance to ionic and oxidative stress, and pathogenicity on wheat. These findings were consistent with previously published data, where, for instance, MoCRZ1 in *P. oryzae* regulates more than 140 genes involved in fungal growth, conidiation, tolerance to ionic stress, and full virulence (Kim et al., 2010). Similarly, FgCrz1A, another homolog of CRZ1, is essential for both fungal growth and virulence in *F. graminearum* (Chen et al., 2019). It was also reported that *A. fumigatus ΔCrzA* deletion mutant exhibited impaired conidiation,

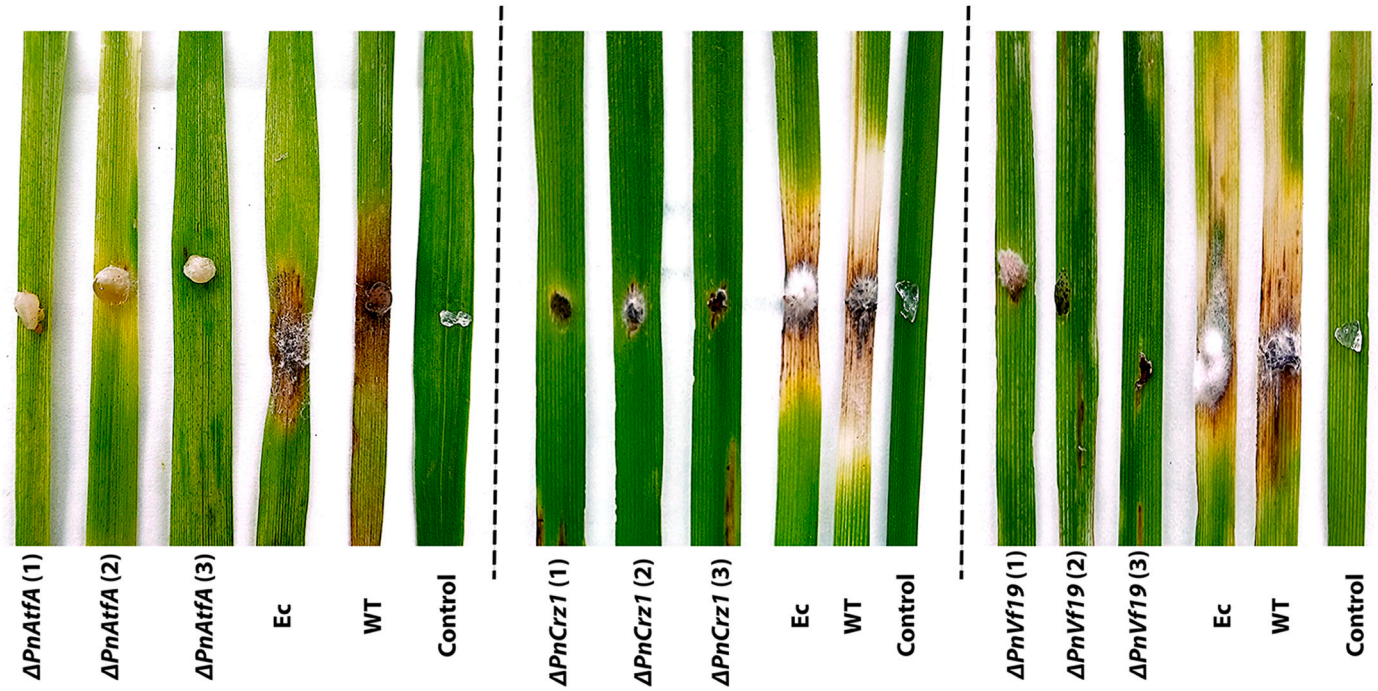

Fig. 7. Detached leaf assay of *Parastagonospora nodorun* Δ*PnAtfA*, Δ*PnCrz1*, and Δ*PnVf19* deletion mutants along with ectopic (Ec) and wild type (WT) strains on wheat cultivar Grandin at 5 days post inoculation (dpi) using mycelial blocks.

increased susceptibility to calcium and manganese ions, and a loss of virulence when compared to the wild-type strain (Soriani et al., 2008). As another example, PdCrz1 was found to be important for conidiation, cell wall integrity, full virulence, and response to stress caused by Ca^{2+} and H_2O_2 in *P. digitatum* (Zhang et al., 2013).

The deletion of *PnCrz1* had the most dramatic impact on the morphology of *P. nodorum* compared to the other candidate TF gene mutants. This morphological alternation includes absence of aerial hyphae, denser hyphal branching, and development of cracks on the colony surface (Fig. 2). The morphological alternation observed in *ΔPnCrz1* deletion mutants is coherent with published data. For instance, deletion of *FgCrz1A* resulted in reduced radial growth, fewer formation of aerial hyphae, and denser hyphal branching in *F. graminearum* (Chen et al., 2019). The *B. cinerea ΔBccrz1* deletion mutant also demonstrated reduced hyphal growth and an abnormal branching pattern (Schumacher et al., 2008). In *A. nidulans*, deletion of *crzA* led to delayed conidial germination and aberrant morphology linked to reduced expression of a chitin synthase gene in the cell wall (Spielvogel et al., 2008).

It was mentioned earlier that CRZ1 provides tolerance to high concentration of Ca^{2+} through regulating the Ca^{2+}/calcineurin signaling pathway (Matheos et al., 1997), which indicates a correlation between calcium signaling pathway and fungal colony morphology. Indeed, alterations in calcium levels or the disruption of calcium-signaling pathway leads to changes in hyphal growth, branching patterns, and development (Zhang et al., 2013). Thus, the explanation to the observed colony morphology defects is likely due to the alteration of the calcium signaling pathway. The involvement of CRZ1 homologs in the maintenance of cell wall structure and/or membrane integrity has been established in several fungi such as *P. oryzae* (Kim et al., 2010), *B. cinerea* (Schumacher et al., 2008), *S. cerevisiae* (Matheos et al., 1997), *A. alternata* (Yang et al., 2022), *P. digitatum* (Zhang et al., 2013), and *A. nidulans* (Spielvogel et al., 2008). Given that cell wall stability is critical for normal penetration and pathogenicity, the reduced virulence observed in *ΔPnCrz1* deletion mutants may be due to a disrupted cell wall stability and/or reduced chitin content. This disruption could lead to less effective mycelial penetration, thus explaining the loss of pathogenicity.

It was mentioned earlier that the TF gene *PnPf2* regulates the expression of NE genes *SnToxA* and *SnTox3* and other virulence-associated genes in *P. nodorum* during infection of wheat (Rybak et al., 2017; Jones et al., 2019). Transcriptome data obtained under *in planta* conditions showed *PnCrz1* was up-regulated in a *PnPf2* deletion mutant (Jones et al., 2019) which means that PnPf2 might acts as a negative regulator of *PnCrz1*. This negative regulation could be directly done through binding of PnPf2 on the promoter of *PnCrz1* because the motif CGATCGTATGGCGTT was found ~850-bp upstream of the *PnCrz1* start codon and closely matches the binding motif CGGCSBYWYBKCGGC of *PnPf2* (John et al., 2024). Considering this regulation, PnCrz1 is unlikely to regulate the expression of *SnToxA* and *SnTox3* and the loss of virulence in *ΔPnCrz1* deletion mutants might not be related to the expression of these NE genes.

PnVf19 was found to share a close homology with the characterized Msn2 in *S. cerevisiae* and had a role in mycelial growth (Fig. 2), sporulation (Fig. 3), oxidative (Fig. 4) and osmotic (Fig. 6) stress tolerance, and pathogenicity (Fig. 7) in *P. nodorum*. These findings are consistent with previous studies elucidating the role of Msn2 homologs in other fungal species. For example, The ZtVf1 is important for pycnidia production and pathogenicity of *Z. tritici* (Mohammadi et al., 2017) with BcMsn2 plays a role in fungal growth, and virulence in *B. cinerea* (Lu et al., 2023). It was also observed that MoMsn2 mediates controlling aerial hyphal growth, appressorium formation, and infection in *P. oryzae* (Zhang et al., 2014) and VdMsn2 contributes to hyphal growth, microsclerotia formation, and virulence in *V. dahliae* (Tian et al., 2017).

PnVf19 has a crucial role in sporulation, and pathogenicity of *P. nodorum*, but no discernible differences in colony morphology were observed between *ΔPnVf19* deletion mutants and WT (Fig. 2). *ΔPnVf19* deletion mutants only showed slower growth. This result is consistent with published data where the TF gene *AbVf19* is associated with the pathogenicity of *A. brassicicola*, yet no significant disparities in fungal vegetative growth were observed between *ΔAbV19* deletion mutants and the wild type (Srivastava et al., 2012).

Msn2 has been reported to play as a general regulator of stress response (Ruis and Schüller, 1995). PnVf19 is required for oxidative and

osmotic stress response by being active against peroxide hydrogen and sodium chloride, respectively. Similar to our finding, it has been suggested that Msn2 homologs are involved in stress response. For instance, MsnA is required for oxidative stress response in two fungal species *A. parasiticus* and *A. flavus* (Chang et al., 2011). Thus, it appears that the ability of *P. nodorum* to deal with oxidative stress during infection of wheat is particularly important.

Atf1 and Msn2 TFs were also shown to regulate the expression of genes responsible for production of cell wall degrading enzymes (CWDEs). This includes regulation of extracellular pectinases, cutinases, and proteinases secretion in *A. brassicicola* by *AbVf19* (Srivastava et al., 2012), and extracellular peroxidases and laccases by *Moatf1* in *P. oryzae* (Guo et al., 2010) and by *VDAG_08676* in *V. dahliae* (Fang et al., 2017). CWDEs are known to degrade plant tissue thus facilitating the pathogen penetration, especially in necrotrophic fungi. Determining the genes regulated by these candidate TFs in *P. nodorum* would provide evidence if down-regulation of CWDEs could also contribute to the lack of pathogenicity of *ΔPnAtfA* and *ΔPnVf19* deletion mutants.

The TF genes selected in our study are known as "general" regulators that are characterized in other fungi and were shown to influence various biological processes which result in defect in pathogenicity in several plant pathogens. In previous studies, the effect on pathogenicity was thus related to general biological processes that impair virulence independently of molecular determinants that are only involved in the pathogenicity process. Because the mutants did not induce any symptom on wheat leaves, the observed loss of virulence is similarly likely due to defect in such general biological process reported in other plant pathogens. Further microscopic analyses of the infection process will be helpful to determine at which stage all three mutants are blocked and whether they show morphological defect on wheat leaves. Yet, we cannot exclude that the selected TFs may also regulate NE genes, and thus might contribute to the loss of virulence. Taken together, as global gene expression regulators, these transcription factors influence a wide range of genes associated with virulence, making it difficult to pinpoint their exact roles in the pathogenicity of plant pathogenic fungi.

5. Conclusion

The work presented here reveals the involvement of three global candidate TF genes *PnAtfA*, *PnCrz1*, and *PnVf19* in fungal morphogenesis, sporulation, abiotic stress tolerance response, and full virulence in *P. nodorum*, one of the most devastating pathogens on wheat. Our results suggest that *P. nodorum* is using conserved signaling pathways to deal with environmental stress, growth and reproduce asexually, and infect host plants. TFs have emerged as promising targets for the management of fungal diseases through gene silencing (John et al., 2021). Small interfering RNAs (siRNAs) and host-induced gene silencing (HIGS) have recently been identified as innovative strategies for developing transgenic plants to manage fungal diseases (Guo et al., 2019). The three candidate TF genes studied here could be considered as potential targets to control *P. nodorum* and mitigate the economic losses caused by this fungal pathogen.

CRediT authorship contribution statement

Roya Choupannejad: Writing – original draft, Visualization, Validation, Software, Methodology, Investigation, Formal analysis, Data curation. **Bahram Sharifnabi:** Writing – review & editing, Supervision, Resources, Project administration, Funding acquisition, Conceptualization. **Jérôme Collemare:** Writing – review & editing, Supervision, Software, Project administration, Methodology, Conceptualization. **Javad Gholami:** Software, Methodology, Formal analysis, Data curation. **Rahim Mehrabi:** Supervision, Project administration, Methodology, Conceptualization.

Declaration of competing interest

All authors declare that they have no conflicts of interest.

Acknowledgment

This research was financially supported by the research council of Isfahan University of Technology (IUT) and Iran National Science Foundation (INSF) with project No. 99007240.

Appendix A. Supplementary data

Supplementary data to this article can be found online at https://doi.org/10.1016/j.funbio.2025.101565.

References

Chang, P.-K., Scharfenstein, L.L., Luo, M., Mahoney, N., Molyneux, R.J., Yu, J., Brown, R. L., Campbell, B.C., 2011. Loss of *msnA*, a putative stress regulatory gene, in *Aspergillus parasiticus* and *Aspergillus flavus* increased production of conidia, aflatoxins and kojic acid. Toxins 3, 82–104.

Chen, L., Tong, Q., Zhang, C., Ding, K., 2019. The transcription factor FgCrz1A is essential for fungal development, virulence, deoxynivalenol biosynthesis and stress responses in *Fusarium graminearum*. Curr. Genet. 65, 153–166.

Chooi, Y.-H., Krill, C., Barrow, R.A., Chen, S., Trengove, R., Oliver, R.P., Solomon, P.S., 2015a. An *in planta*-expressed polyketide synthase produces (R)-mellein in the wheat pathogen *Parastagonospora nodorum*. Appl. Environ. Microbiol. 81, 177–186.

Chooi, Y.-H., Muria-Gonzalez, M.J., Mead, O.L., Solomon, P.S., 2015b. SnPKS19 encodes the polyketide synthase for alternariol mycotoxin biosynthesis in the wheat pathogen *Parastagonospora nodorum*. Appl. Environ. Microbiol. 81, 5309–5317.

Choupannejad, R., Sharifnabi, B., Mehrabi, R., Gholami, J., Massah, A., Collemare, J., 2023. Specific up-regulation of transcription factors in the fungus *Parastagonospora nodorum* suggests a role in pathogenicity on wheat. Mycol. Iranica. 10, 79–88.

Duba, A., Goriewa-Duba, K., Wachowska, U., 2018. A review of the interactions between wheat and wheat pathogens: *Zymoseptoria tritici, Fusarium* spp. and *Parastagonospora nodorum*. Int. J. Mol. Sci. 19, 1138.

Fang, Y., Xiong, D., Tian, L., Tang, C., Wang, Y., Tian, C., 2017. Functional characterization of two bZIP transcription factors in *Verticillium dahliae*. Gene 626, 386–394.

Guo, M., Guo, W., Chen, Y., Dong, S., Zhang, X., Zhang, H., Song, W., Wang, W., Wang, Q., Lv, R., 2010. The basic leucine zipper transcription factor Moatf1 mediates oxidative stress responses and is necessary for full virulence of the rice blast fungus *Magnaporthe oryzae*. Mol. Plant Microbe Interact. 23, 1053–1068.

Guo, X.-Y., Li, Y., Fan, J., Wang, W.-M., 2019. Host-induced gene silencing of *MoAP1* confers broad-spectrum resistance to *Magnaporthe oryzae*. Front. Plant Sci. 10, 431831.

Hirayama, S., Sugiura, R., Lu, Y., Maeda, T., Kawagishi, K., Yokoyama, M., Tohda, H., Giga-Hama, Y., Shuntoh, H., Kuno, T., 2003. Zinc finger protein Prz1 regulates Ca^{2+} but not Cl^{-} homeostasis in fission yeast: identification of distinct branches of calcineurin signaling pathway in fission yeast. J. Biol. Chem. 278, 18078–18084.

Ipcho, S.V., Hane, J.K., Antoni, E.A., Ahren, D., Henrissat, B., Friesen, T.L., Solomon, P. S., Oliver, R.P., 2012. Transcriptome analysis of *Stagonospora nodorum*: gene models, effectors, metabolism and pantothenate dispensability. Mol. Plant Pathol. 13, 531–545.

IpCho, S.V., Tan, K.-C., Koh, G., Gummer, J., Oliver, R.P., Trengove, R.D., Solomon, P.S., 2010. The transcription factor StuA regulates central carbon metabolism, mycotoxin production, and effector gene expression in the wheat pathogen *Stagonospora nodorum*. Eukaryot. Cell 9, 1100–1108.

John, E., Lopez-Ruiz, F., Rybak, K., Mousley, C.J., Oliver, R.P., Tan, K.-C., 2016. Dissecting the role of histidine kinase and HOG1 mitogen-activated protein kinase signalling in stress tolerance and pathogenicity of *Parastagonospora nodorum* on wheat. Microbiol. 162, 1023–1036.

John, E., Singh, K.B., Oliver, R.P., Tan, K.C., 2021. Transcription factor control of virulence in phytopathogenic fungi. Mol. Plant Pathol. 22, 858–881.

John, E., Verdonk, C., Singh, K.B., Oliver, R.P., Lenzo, L., Morikawa, S., Soyer, J.L., Muria-Gonzalez, J., Soo, D., Mousley, C., Jacques, S., Tan, K.C., 2024. Regulatory insight for a Zn2Cys6 transcription factor controlling effector-mediated virulence in a fungal pathogen of wheat. PLoS Pathog. 20, e1012536.

Jones, D.A., John, E., Rybak, K., Phan, H.T., Singh, K.B., Lin, S.-Y., Solomon, P.S., Oliver, R.P., Tan, K.-C., 2019. A specific fungal transcription factor controls effector gene expression and orchestrates the establishment of the necrotrophic pathogen lifestyle on wheat. Sci. Rep. 9, 15884.

Kim, S., Hu, J., Oh, Y., Park, J., Choi, J., Lee, Y.-H., Dean, R.A., Mitchell, T.K., 2010. Combining ChIP-chip and expression profiling to model the MoCRZ1 mediated circuit for Ca^{2+}/calcineurin signaling in the rice blast fungus. PLoS Pathog. 6, e1000909.

Lin, S.-Y., 2017. The Study of Transcriptional Regulation of Necrotrophic Effector Genes *ToxA* and *Tox3* in the Wheat Pathogen *Parastagonospora Nodorum*, Ph.D. Dissertation. Australian National University., Canberra.

Lin, S.-Y., Chooi, Y.H., Solomon, P.S., 2018. The global regulator of pathogenesis PnCon7 positively regulates *Tox3* effector gene expression through direct interaction in the wheat pathogen *Parastagonospora nodorum*. Mol. Microbiol. 109, 78–90.

Lowe, R.G., Lord, M., Rybak, K., Trengove, R.D., Oliver, R.P., Solomon, P.S., 2008. A metabolomic approach to dissecting osmotic stress in the wheat pathogen *Stagonospora nodorum*. Fungal Genet. Biol. 45, 1479–1486.

Lu, P., Wang, K., Wang, J., Xia, C., Yang, S., Ma, L., Shi, H., 2023. A novel zinc finger transcription factor, BcMsn2, is involved in growth, development, and virulence in *Botrytis cinerea*. Front. Microbiol. 14, 1247072.

Luo, X., Zhan, X., Ruan, R., Xi, Y., Shen, C., Wang, H., Wang, M., 2022. Genome-wide identification of the *Penicillium digitatum* bZIP gene family and the roles of one key member, *PdatfA*. Res. Microbiol. 173, 103970.

Matheos, D.P., Kingsbury, T.J., Ahsan, U.S., Cunningham, K.W., 1997. Tcn1p/Crz1p, a calcineurin-dependent transcription factor that differentially regulates gene expression in *Saccharomyces cerevisiae*. Genes Dev. 11, 3445–3458.

Mehrabi, R., Gohari, A.M., da Silva, G.F., Steinberg, G., Kema, G.H., de Wit, P.J., 2015. Flexible gateway constructs for functional analyses of genes in plant pathogenic fungi. Fungal Genet. Biol. 79, 186–192.

Mohammadi, N., Mehrabi, R., Gohari, A.M., Goltapeh, E.M., Safaie, N., Kema, G.H., 2017. The ZtVf1 transcription factor regulates development and virulence in the foliar wheat pathogen *Zymoseptoria tritici*. Fungal Genet. Biol. 109, 26–35.

Nathues, E., Joshi, S., Tenberge, K.B., von den Driesch, M., Oeser, B., Bäumer, N., Mihlan, M., Tudzynski, P., 2004. CPTF1, a CREB-like transcription factor, is involved in the oxidative stress response in the phytopathogen *Claviceps purpurea* and modulates ROS level in its host *Secale cereale*. Mol. Plant Microbe Interact. 17, 383–393.

Oliver, R.P., Friesen, T.L., Faris, J.D., Solomon, P.S., 2012. *Stagonospora nodorum*: from pathology to genomics and host resistance. Annu. Rev. Phytopathol. 50, 23–43.

Peters Haugrud, A.R., Zhang, Z., Friesen, T.L., Faris, J.D., 2022. Genetics of resistance to septoria nodorum blotch in wheat. Theor. Appl. Genet. 1–23.

Ruis, H., Schüller, C., 1995. Stress signaling in yeast. Bioessays 17, 959–965.

Rybak, K., See, P.T., Phan, H.T., Syme, R.A., Moffat, C.S., Oliver, R.P., Tan, K.C., 2017. A functionally conserved Zn2Cys6 binuclear cluster transcription factor class regulates necrotrophic effector gene expression and host-specific virulence of two major Pleosporales fungal pathogens of wheat. Mol. Plant Pathol. 18, 420–434.

Schmittgen, T.D., Livak, K.J., 2008. Analyzing real-time PCR data by the comparative CT method. Nature protoc 3, 1101–1108.

Schumacher, J., de Larrinoa, I.F., Tudzynski, B., 2008. Calcineurin-responsive zinc finger transcription factor CRZ1 of *Botrytis cinerea* is required for growth, development, and full virulence on bean plants. Eukaryot. Cell 7, 584–601.

Solomon, P.S., Ipcho, S.V., Hane, J.K., Tan, K.-C., Oliver, R.P., 2008. A quantitative PCR approach to determine gene copy number. Fungal Genet. Rep. 55, 5–8.

Solomon, P.S., Lee, R.C., Wilson, T.G., Oliver, R.P., 2004a. Pathogenicity of *Stagonospora nodorum* requires malate synthase. Mol. Microbiol. 53, 1065–1073.

Solomon, P.S., Tan, K.-C., Sanchez, P., Cooper, R.M., Oliver, R.P., 2004b. The disruption of a Gα subunit sheds new light on the pathogenicity of *Stagonospora nodorum* on wheat. Mol. Plant Microbe Interact. 17, 456–466.

Song, M., Fang, S., Li, Z., Wang, N., Li, X., Liu, W., Zhang, Y., Lin, C., Miao, W., 2022. CsAtf1, a bZIP transcription factor, is involved in fludioxonil sensitivity and virulence in the rubber tree anthracnose fungus *Colletotrichum siamense*. Fungal Genet. Biol. 158, 103649.

Soriani, F.M., Malavazi, I., da Silva Ferreira, M.E., Savoldi, M., Von Zeska Kress, M.R., de Souza Goldman, M.H., Loss, O., Bignell, E., Goldman, G.H., 2008. Functional characterization of the *Aspergillus fumigatus* CRZ1 homologue. CrzA. Mol. Microbiol. 67, 1274–1291.

Spielvogel, A., Findon, H., Arst Jr, H.N., Araújo-Bazán, L., Hernández-Ortíz, P., Stahl, U., Meyer, V., Espeso, E.A., 2008. Two zinc finger transcription factors, CrzA and SltA, are involved in cation homoeostasis and detoxification in *Aspergillus nidulans*. Biochem. J. 414, 419–429.

Srivastava, A., Ohm, R.A., Oxiles, L., Brooks, F., Lawrence, C.B., Grigoriev, I.V., Cho, Y., 2012. A zinc-finger-family transcription factor, *AbVf19*, is required for the induction of a gene subset important for virulence in *Alternaria brassicicola*. Mol. Plant Microbe Interact. 25, 443–452.

Szabó, Z., Pákozdi, K., Murvai, K., Pusztahelyi, T., Kecskeméti, Á., Gáspár, A., Logrieco, A.F., Emri, T., Ádám, A.L., Leiter, É., 2020. *FvatfA* regulates growth, stress tolerance as well as mycotoxin and pigment productions in *Fusarium verticillioides*. Appl. Microbiol. Biotechnol. 104, 7879–7899.

Tamura, K., Stecher, G., Kumar, S., 2021. MEGA11: molecular evolutionary genetics analysis version 11. Mol. Biol. Evol. 38, 3022–3027.

Temme, N., Oeser, B., Massaroli, M., Heller, J., Simon, A., Gonzalez Collado, I., Viaud, M., Tudzynski, P., 2012. BcAtf1, a global regulator, controls various differentiation processes and phytotoxin production in *Botrytis cinerea*. Mol. Plant Pathol. 13, 704–718.

Tian, L., Yu, J., Wang, Y., Tian, C., 2017. The C2H2 transcription factor VdMsn2 controls hyphal growth, microsclerotia formation, and virulence of *Verticillium dahliae*. Fungal Biol. 121, 1001–1010.

Van Nguyen, T., Kröger, C., Bönnighausen, J., Schäfer, W., Bormann, J., 2013. The ATF/CREB transcription factor Atf1 is essential for full virulence, deoxynivalenol production, and stress tolerance in the cereal pathogen *Fusarium graminearum*. Mol. Plant Microbe Interact. 26, 1378–1394.

Wilkinson, M.G., Samuels, M., Takeda, T., Toone, W.M., Shieh, J.-C., Toda, T., Millar, J., Jones, N., 1996. The Atf1 transcription factor is a target for the Sty1 stress-activated MAP kinase pathway in fission yeast. Genes Dev. 10, 2289–2301.

Yang, Y., Xie, P., Yuan, J., Liu, Y., Zhang, M., Li, Y., Bi, Y., Prusky, D.B., 2022. The calcineurin-responsive transcription factor *Crz1* is required for regulation of infection structure differentiation, calcium homeostasis and cell wall integrity in *Alternaria alternata*. Postharvest Biol. Technol. 194, 112064.

Zhang, H., Zhao, Q., Guo, X., Guo, M., Qi, Z., Tang, W., Dong, Y., Ye, W., Zheng, X., Wang, P., 2014. Pleiotropic function of the putative zinc-finger protein MoMsn2 in *Magnaporthe oryzae*. Mol. Plant Microbe Interact. 27, 446–460.

Zhang, T., Xu, Q., Sun, X., Li, H., 2013. The calcineurin-responsive transcription factor Crz1 is required for conidation, full virulence and DMI resistance in *Penicillium digitatum*. Microbiol. Res. 168, 211–222.